

Thermal stability and spectroscopic studies of zemkorite: A carbonate from the Venkatampalle kimberlite of southern India

G. PARTHASARATHY,^{1,*} T.R.K. CHETTY,¹ AND S.E. HAGGERTY²

¹National Geophysical Research Institute, Uppal Road, Hyderabad-500 007, India

²Department of Geosciences, University of Massachusetts, Amherst, Massachusetts 01003, U.S.A.

ABSTRACT

While characterizing the mineralogy of the kimberlite at Venkatampalle, Andhra Pradesh, India (Lat. 14° 56' 00" N, Long. 77° 22' 15" E), we found the second occurrence of zemkorite (Na,K)₂Ca(CO₃)₂, which was first reported in 1989 in the Udachnaya kimberlite in Siberia. We also report the first Fourier-transform infrared spectroscopic (FTIR), scanning electron microscopic, thermo-gravimetric, and high-temperature heat capacity measurements on this rare carbonate. Powder X-ray diffraction (XRD) patterns show 24 well-resolved diffraction lines, all of which can be indexed with a hexagonal cell with $a = 10.038(5)$ Å and $c = 12.726(5)$ Å. The vibrational spectrum of zemkorite at room temperature exhibits 13 distinct absorption bands in the frequency range 2000 to 400 cm⁻¹. The IR bands of zemkorite indicate a structural similarity with shortite but are quite distinct from other alkali carbonates such as nyerereite, butschiiite, and fairchildite. The heat capacity of zemkorite has been measured up to 700 K by differential scanning calorimetric techniques. The temperature dependence of the heat capacity of zemkorite was fitted with the polynomial $C_p = 140.2 + 8.584 \times 10^{-2} T - 2.458 \times 10^{-6} T^2$. The upper thermal stability of zemkorite is ~700 K, which is similar to shortite. Zemkorite may have formed during the late stages of kimberlite genesis, possibly as a result of metasomatism or by the breakdown of metasomatic natrocarbonatitic minerals or glass that segregated on decompression melting in the upper mantle.

INTRODUCTION

Zemkorite was previously described from the Udachnaya pipe, Daldyn kimberlite field, Yakutia, Russia (Yegorov et al. 1988; Jambor and Grew 1990). The mineral was discovered in core samples at a depth of 400–450 m in the eastern part of the pipe. Zemkorite occurs in thin fractures in unaltered kimberlite and along contacts between the kimberlite groundmass and olivine xenoliths and xenocrysts, where the mineral is associated with shortite and halite. To the best of our knowledge no other occurrences of zemkorite have been reported, and there are no spectroscopic, heat capacity, or thermal stability data for the mineral. The new occurrence of this rare carbonate is supported by X-ray diffraction, infrared spectroscopic, high-temperature heat capacity, differential thermal analysis (DTA), and thermo-gravimetric (TG) data.

GEOLOGICAL SETTING

A dike-like kimberlite body, discovered by heavy mineral stream sediment sampling (Guptasarma et al. 1986) and designated Pipe-7, is the richest diamondiferous kimberlite in the Wajrakarur Kimberlite Province of South India. Pipe-7 is located ~15 km south of the village of Wajrakarur (Lat. 14° 56' 00" N, Long. 77° 22' 15" E). The dike is one of a cluster of 18 kimberlites within a radius of 50 km (Fig. 1). Pipe-7 is ~1100

Ma (Kumar et al. 1993), and it intrudes the Archean granite-greenstone sequence of the Eastern Dharwar Craton. The body occurs in the central part of the Penakacherla schist belt, which is highly sheared and intruded by younger granites. Pipe-7, however, is in a low strain domain where amphibolites exhibit unusually well preserved pillow structures.

Pipe-7 strikes ENE-WSW and extends discontinuously for a length of ~1.5 km in the form of several "blows." The maximum width is 27 m and the kimberlite body dips steeply (80 degrees) toward the south (Fig. 2). Structurally, the pipe occurs near the intersection of NNW-SSE trending major shear zones and ENE-WSW striking cross faults. The emplacement of the pipe has been attributed to block rotation tectonics (Chetty 1995), which explains the emplacement along a splay fault close to the intersection.

The kimberlite contains subangular to rounded xenoliths of mantle-derived peridotites, garnet pyroxenites, and eclogites, as well as crustal fragments of amphibolites and granites. Petrographically, the kimberlite is characterized by euhedral and subhedral altered olivine, phlogopite, clinopyroxene, garnet, chromite, ilmenite, and perovskite, with associated serpentine, chlorite, amphibole, calcite, and clay minerals (Rao and Charan 1993). This pipe has been classified as a monticellite-bearing mica rich (Group I) kimberlite with similarities to many of the diamondiferous kimberlites in South Africa. Coexisting ilmenite-magnetite compositions from the pipe show a tempera-

* E-mail: gpngri@rediffmail.com

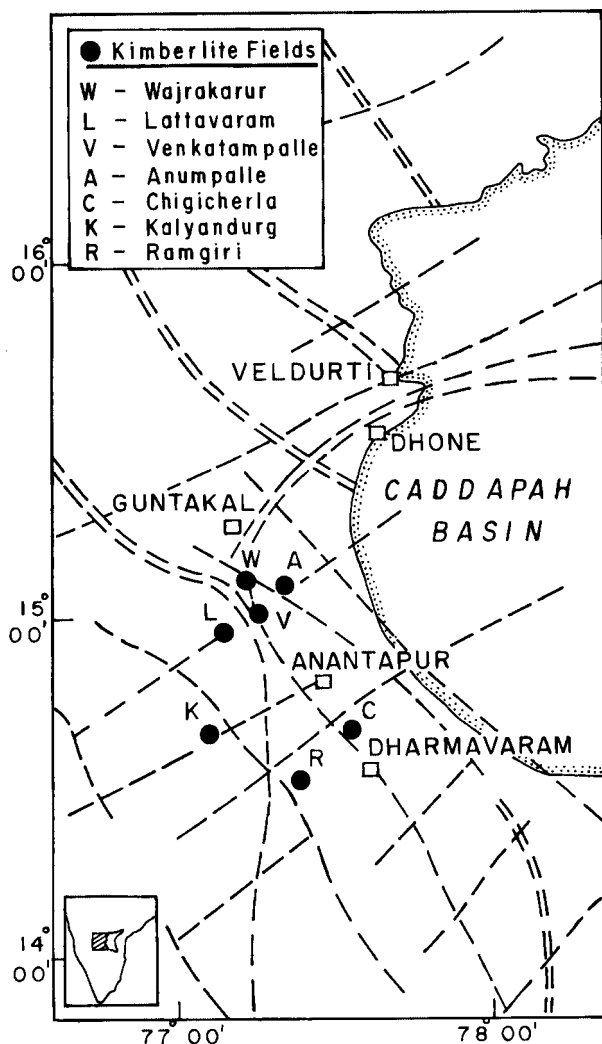


FIGURE 1. Map showing kimberlite occurrences and their associations with major shear zones.

ture of 1200 ± 50 °C and a $\log f_{O_2}$ value of -8.3 (Mukherjee 2000), which, on extrapolation to high pressures, lies between iron-wustite (IW) and (WM) wustite-magnetite (Haggerty 1986). Chemical composition and thermodynamic properties of Mg-rich garnets indicate that the kimberlite was exhumed from the diamond stability field (Parthasarathy et al. 2001). Large scale depletion ($\sim 20\%$) of the source regions, with subsequent carbonatitic enrichment (Haggerty 1989) in large-ion-lithophile-elements (K, Na, Ba, Sr, REE) and high-field-strength-elements (Ti, Zr, Nb, P), are considered prerequisites for the generation of kimberlites and lamproites of South India (Chalapathi Rao 1998).

The samples considered in this study were collected from friable yellow ground at a depth of ~ 4 m (Fig. 2); tough hardbank (blue ground) occurs at ~ 10 m. The kimberlite is coarsely brecciated and unevenly mixed with xenolithic rock fragments and xenolithic minerals. The samples consist of altered grains of olivine, phlogopite, and indicator minerals such

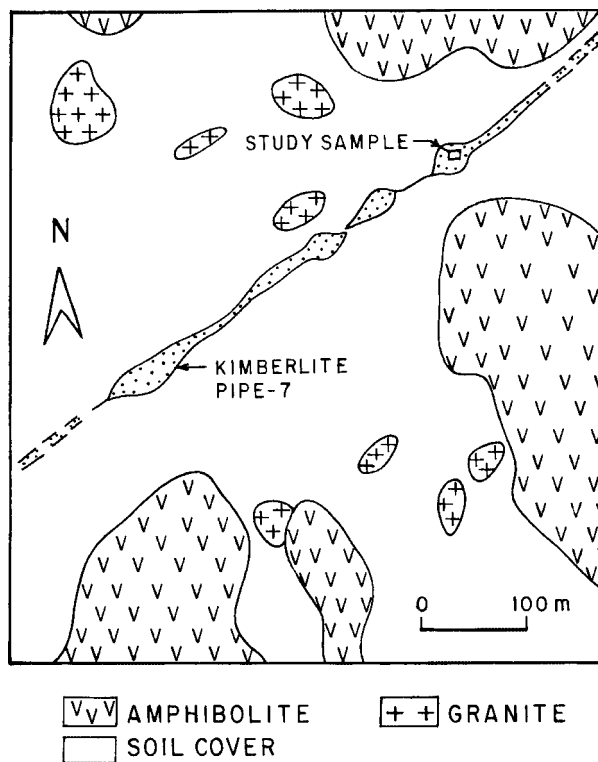


FIGURE 2. Geological map showing different rock formation around the kimberlite Pipe-7.

as pyrope garnet with kelyphitic rims, microilmenite with “leucoxene” skins, chrome-diopside, and an unidentified cream-colored mineral that we now know to be zemkorite.

ANALYTICAL TECHNIQUES

Zemkorite was separated by hand picking under a binocular microscope. Electron microbeam analyses of zemkorite were obtained with an automated CAMECA Camebax SX50 instrument with an accelerating voltage of 15 kV, a beam current of 3.3 nA, and a beam diameter of 1–2 micrometers. Qualitative compositions of zemkorite were also determined with a Hitachi S-520 scanning electron microscope, in EDAX mode with a filament current of 110 microamperes and an accelerating voltage of 20 kV.

Powder X-ray diffraction (XRD) studies were carried out using a Siemens D5000 powder diffractometer with a HOPG graphite monochromator. $CuK\alpha$ radiation with a wavelength of 1.5406 \AA was used in all the diffraction experiments.

Differential thermal analysis and thermogravimetry studies were carried out with a Mettler Toledo Star system, using a 20 mg sample and a heating rate of 20 K/min. The composition of the gas liberated by thermal reaction was analyzed with a mass spectrometer.

Fourier Transform Infrared (FTIR) spectra were recorded in transmission mode, using KBr pressed disks and Nicolet and BIORAD FTIR spectrophotometers. The Nicolet instrument

was purged with dry CO₂-free air and a blank KBr disk was used to generate the background, which was automatically subtracted from sample spectra. The resolution of a spectrum was typically 2 cm⁻¹. All spectra were recorded over the frequency range 4000–200 cm⁻¹.

Heat capacity measurements were carried out up to 700 K with a computer-controlled Perkin-Elmer model DSC-7 differential scanning calorimeter, using the DSC-7 Kinetics program, with a heating rate of 10 K/min and a range setting of 1.5 J/min (Parthasarathy et al. 2001). All samples were encapsulated in standard aluminum pans and weighed on a microbalance. The DSC cell was heated by platinum resistance heaters and the temperature was measured with platinum temperature sensors. Temperature precision and accuracy are ±0.1 K, and the calorimetric precision was better than ±0.1% (Parthasarathy et al. 2001). The accuracy of the DSC data was determined by comparison to the heat capacities of corundum and spinel published by Robie et al. (1978) and Navrotsky (1995).

RESULTS AND DISCUSSION

Zemkorite occurs as translucent and acicular aggregates. At higher magnifications and under SEM, the aggregates are resolved into well ordered fan-shaped arrays (Fig. 3), which are also described, but only rarely, in the Udachnaya occurrence.

Composition

The chemical compositions of three grains of zemkorite from the Venkatampalle kimberlite are listed in Table 1. Each grain was analyzed at six different points. The analyses of the Pipe-7 sample, when compared with zemkorite from Udachnaya (Table 1), show that the two samples, with the exception of the presence of minor MnO and FeO in the former, are very similar. The average CO₂ content (measured with the DTA/TG in situ mass analyzer) is 39.20 wt%. The composition of zemkorite from Pipe-7 corresponds to (Na_{1.765}K_{0.294})Ca_{1.076}C_{1.9471}O_{5.992} with Na/K = 6.003, which is close to the ideal composition of (Na,K)₂Ca(CO₃)₂ (Jambor and Grew 1990).

X-ray diffraction

Powder XRD studies of the zemkorite sample yielded 26 well-resolved diffraction peaks, and all were indexed with a hexagonal cell with unit-cell parameters $a = 10.038(5)$ Å and $c = 12.726(5)$ Å. Diffraction lines along with the interplanar spacing, intensity, and indexing are listed in Table 2. These results are compared with those of the Udachnaya zemkorite ($a = 10.06$ Å; $c = 12.72$ Å) in Table 2. Overall, there is good agreement, although we did not observe the XRD peak at 3.08 Å, which was present in Yakutian sample (40% relative intensity). This line is a non-Bragg reflection, which could be due to the presence of minor amounts of natrofairchildite. In our sample, weak Bragg reflections at 2.92, 2.68, 1.677 Å, which were reported in Yakutian zemkorite, are also absent. The reasons for the absence of these reflections are not known.

DTA and TG

Figure 4 shows DTA and TG spectra for zemkorite from Pipe-7 up to 750 K. The zemkorite samples exhibit a strong

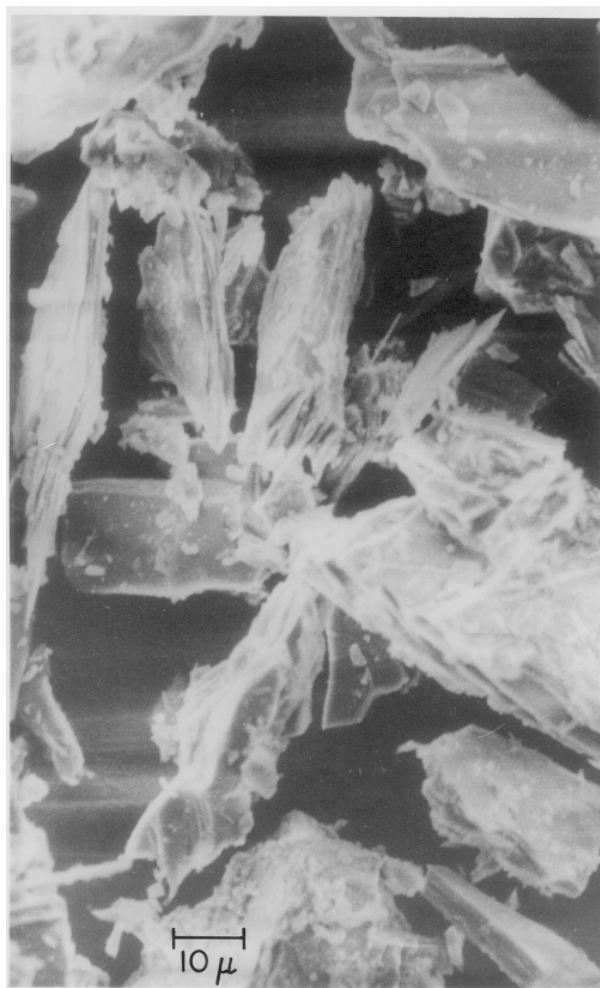


FIGURE 3. Scanning electron microscopic images of zemkorite exhibiting a fan shaped morphology. Scale bar = 10 micrometers.

TABLE 1. Electron microprobe analyses (oxide wt%) of three different grains of zemkorite

Oxides	Sample 1	Sample 2	Sample 3	Average	YUKBS
Na ₂ O	25.20	25.68	25.45	25.44	25.72
Al ₂ O ₃	0.10	0.07	0.06	0.077	0.05
K ₂ O	6.72	6.12	6.42	6.42	6.40
CaO	27.96	28.10	28.12	28.06	28.39
MnO	0.02	0.01	0.00	0.01	0.00
FeO	0.03	0.03	0.03	0.03	0.00
CO ₂				39.84	39.20

Notes: Each column represents the average of 6 different analyses. The last column represents the average composition of the Udachnaya zemkorite (YUKBS) (Yegorov et al. 1988). The number of ions is based on six O atoms per formula unit. Na = 1.765; K = 0.294; Ca = 1.076; C = 1.947 ignoring the minor amounts of Al, Mn, and Fe in the samples.

endothermic peak at about 670 K accompanied by about 36 wt% loss. The composition of the liberated gas was analyzed by in situ mass spectroscopy and found to contain only CO₂. The present high-temperature DTA and TG studies show that zemkorite is stable up to 670 K, which is very close to the upper stability limit of shortite in the presence of excess calcite (673 K), and is much higher than pure shortite, which de-

TABLE 2. Powder X-ray diffraction data for zemkorite: Present study (PC) and the Udachanya sample (YUKBS) (Yegorov et al. 1988)

	$d(\text{\AA})$	l	(hkl)
PC	YUKB		
06.363	06.36	90	(002)
04.347	04.36	100	(200)
04.113	04.13	40	(201)
03.812	03.80	30	(103)
03.589	03.59	30	(202)
03.181	03.18	60	(004), (211)
-	03.08	40	-
03.036	03.04	100	(203)
02.988	02.98	20	(104)
02.598	02.61	20	(213)
02.567	02.57	40	(204)
02.510	02.52	100	(220)
02.442	02.43	20	(105), (130)
02.334	02.34	20	(222)
02.173	02.18	70	(400)
02.142	02.14	40	(401)
02.121	02.12	40	(006)
02.058	02.06	100	(402), (106)
01.954	01.954	20	(116)
01.934	01.938	30	(403)
01.903	01.907	40	(232)
01.818	01.817	40	(412)
01.795	01.797	80	(404)
01.690	01.692	40	(234)
01.629	01.634	20	(414)
01.620	01.621	20	(226)
01.591	01.593	40	(242)

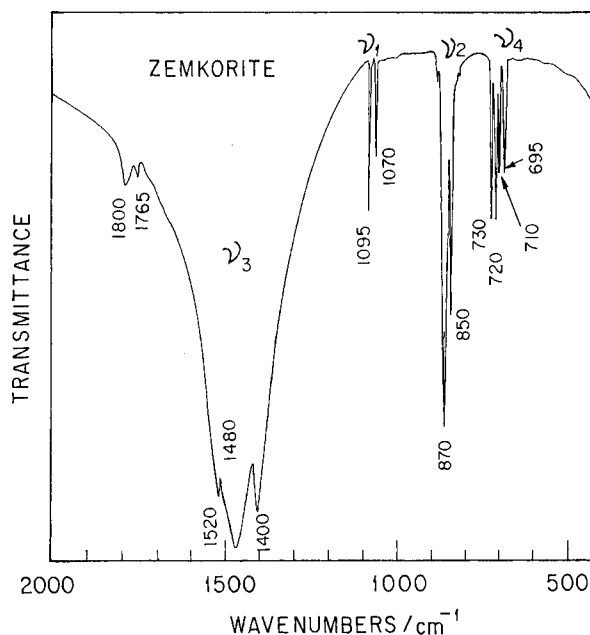


FIGURE 5. FTIR spectrum of zemkorite. The mode assignments are discussed in the text.

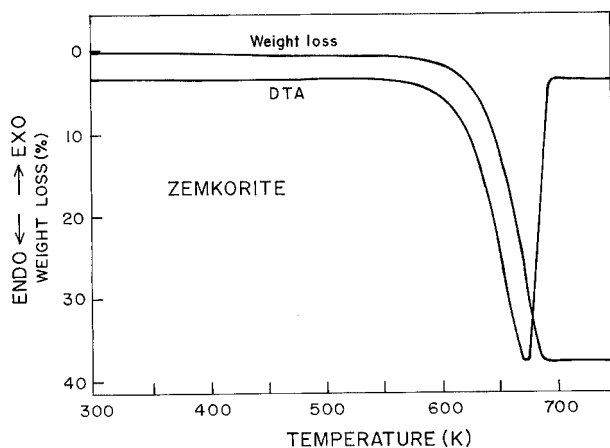


FIGURE 4. Differential thermal analysis (DTA) and thermogravimetric (TG) traces of zemkorite up to 750 K. The endothermic peak at about 670 K with 36 wt% weight loss is attributed to decarbonation.

TABLE 3. Infrared absorption frequencies (in cm⁻¹) for zemkorite and comparison with those of shortite and nyerereite (in the frequency range 2000–400 cm⁻¹)

zemkorite	shortite	nyerereite
1800	1808	1795
1765	1765	-
1520	1521	-
1480	1481	1468
	1453	-
1400	1401	-
1095	1090	1186, 1144, 1108
1070	1071	1079, 1010
870	872	873
	866	-
850	851	-
730	731	-
720	719	-
710	710	710
695	694	689
-	-	648
-	-	622
-	-	573

Note: The FTIR data for shortite and nyerereite are taken from Jones and Jackson (1993).

composes at 610 K (Watkinson and Chao 1973; Cooper and Gittins 1974).

Infrared spectroscopy

A transmission FTIR spectrum of the Pipe-7 zemkorite is shown in Figure 5. As the sample did not show any hydroxyl bands in the frequency range 2000–4000 cm⁻¹, the FTIR spectrum is presented only for the frequency range 2000–400 cm⁻¹. The frequencies of the IR bands are listed in Table 3, and they are compared with published IR data for shortite and nyerereite (White 1974; Jones and Jackson 1993). The carbonate structure contains isolated CO₃²⁻ groups. The vibrational mode as-

signments of CO₃²⁻ ion are discussed by several workers (Konovalov and Solomonik 1983; McMillan and Hofmeister 1988). The free CO₃²⁻ ion has six vibrational modes: a symmetric stretching vibration (ν₁); an out of plane bend (ν₂); a doubly degenerate symmetric stretch (ν₃); and a doubly degenerate bending mode (ν₄). We have interpreted the FTIR data on zemkorite by comparing the spectra of corresponding well studied carbonate minerals such as calcite and dolomite (McMillan and Hofmeister 1988). Figure 5 and Table 3 show that most of the observed IR bands of zemkorite are quite distinct from the FTIR data of other alkali carbonates such as shortite and nyerereite. However the FTIR spectrum of zemkorite has many

features similar to the shortite spectrum. Strong IR bands near 1480 cm^{-1} are assigned to the CO_3^{2-} asymmetric stretching vibrational mode, the peaks near 850 and 870 cm^{-1} are assigned to the CO_3^{2-} out-of-plane bending mode, and IR bands in $695\text{--}730\text{ cm}^{-1}$ region are assigned to the CO_3^{2-} in-plane bending mode. The in-plane bending mode is doubly degenerate for undistorted carbonate groups, but as the carbonate groups become distorted from regular planar symmetry, it splits into many components (McMillan and Hofmeister 1988). The appearance of two strong ν_1 bands at 1095 and 1070 cm^{-1} shows that there must be at least two crystallographically distinct carbonate ions in the zemkorite structure. This is supported by the separation of ν_4 into four distinct peaks at 730 , 720 , 710 , and 695 cm^{-1} . As lifting the degeneracy produces a pair of modes, two quite different carbonate ions are required to produce four modes. However, further studies on single-crystal X-ray diffraction are needed to understand the crystal structure of this novel carbonate.

Heat capacity

Carbonates are potentially significant hosts for primordial and subducted carbon in the Earth's mantle (Barker 1996). High-pressure and high-temperature powder X-ray diffraction and Raman spectroscopic studies of aragonite and dolomite show that these carbonates are stable to at least 9 GPa and 1070 K , indicating that carbon is stably bound within carbonate phases in the entire upper mantle and shallow lower mantle (Kraft et al. 1991; Luth 2001). Hence, studies of the thermodynamic properties of carbonates are essential to estimate their phase stability under mantle conditions, and heat capacity is an important parameter. However, there are few measurements on carbonates and these are limited to calcite, magnesite, and dolomite (Robie et al. 1978; Navrotsky 1995). The heat capacity of other carbonates is usually estimated by theoretical calculations using the well-known Hazen (1985) basic polyhedral unit model (Holland and Powell 1990; La Iglesia and Felix 1994). Figure 6 shows the temperature dependence of the heat capacity of zemkorite up to 700 K . We could not collect any DSC data above 700 K due to decomposition of the carbonate. The temperature of the phase transformation as measured by DSC is 30 K higher than that measured in the DTA/TG studies (Fig. 4). This higher value could be due to differences in heating rates and sample size between the two experiments, because the kinetics of the thermal transformation depends upon the heating rate as well as the weight of the sample. The experimental data were fitted to the standard polynomial $C_p = 140.2 + 8.584 \times 10^{-2} T - 2.458 \times 10^{-6} T^2$, where C_p is the heat capacity in $\text{J}/(\text{K}\cdot\text{mol})$ and T is the temperature in degrees Kelvin. The values of heat capacity for zemkorite lie between the values for calcite and dolomite (Fig. 6).

Genesis

Zemkorite was identified as a post-magmatic mineral in the Udachnaya pipe and was considered to have formed by alteration of kimberlite and interaction with highly mineralized solutions that were unusually rich in sodium (Yegorov et al. 1988). Although we do not have the precise textural context of zemkorite in Pipe-7, there is no field evidence in the South Indian setting for the interaction of kimberlite with brines. The

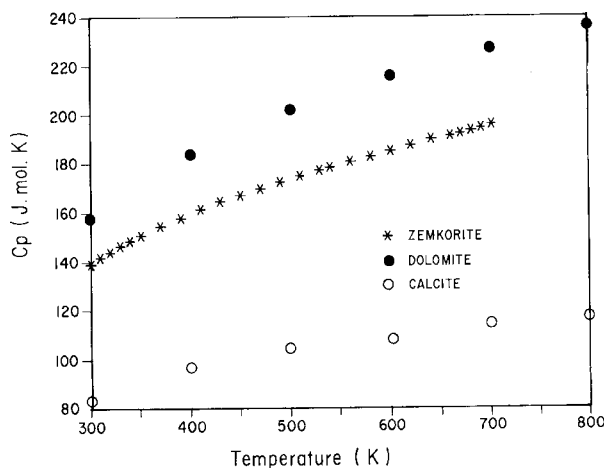


FIGURE 6. Temperature dependence of the heat capacity of zemkorite.

concentration of potassium is typically much higher than sodium in kimberlites, and sodium in mantle-derived melts is more typically associated with carbonatites (Bell 1989; Haggerty 1989). The major host mineral for sodium in the upper mantle is the jadeite ($\text{NaAlSi}_2\text{O}_6$) component of clinopyroxene, specifically diopside ($\text{CaMgSi}_2\text{O}_6$); in these minerals, the resulting solid solution (omphacite) may contain up to $70\text{ mol}\%$ jadeite (Haggerty 1995). It is noteworthy that there are also rare inclusions of brine in diamond with associated carbonates (Israeli et al. 2001). Carbonate metasomatism is pervasive in kimberlites and lamproites (Haggerty 1989, 1995) and is invoked in the formation of omphacitic inclusions in diamonds (Gasparik and Hutchinson 2000), and of trapped melts in coated diamonds (Schrauder et al. 1994). Immiscible, natrosilicic, and carbonatitic conjugate melts are described in metasomatized mantle eclogites (Pyle and Haggerty 1994), with major concentrations of Na_2O in natrolite ($16\text{ wt}\%$), pectolite ($9\text{ wt}\%$), and devitrified glass ($9\text{--}14\text{ wt}\%$). Because zemkorite is dominantly sodic, but with significant Ca, and a carbonate, we propose that the mineral formed during the late stages of kimberlite genesis by decompression melting and liquid immiscible separation of a natrocarbonate melt. Our estimate of 700 K for the upper thermal stability limit of zemkorite does not greatly exceed the thermal stabilities of Na-K-Ca carbonate mineral solid solutions in the pure $\text{Na}_2\text{CO}_3\text{--K}_2\text{CO}_3\text{--CaCO}_3$ system (Cooper et al. 1975), and is comparable to the estimates made by Pyle and Haggerty (1994) for upper mantle eclogites. Cooper and Gittins (1974) explained the presence of shortite, $\text{Na}_2\text{Ca}_2(\text{CO}_3)_3$, in the matrix of a kimberlite from Canada, as the result of the subsolidus breakdown of nyerereite $\text{Na}_2\text{Ca}(\text{CO}_3)_2$. We find no evidence for these minerals, or for gregoryite, $(\text{Na}_2, \text{K}_2, \text{Ca})(\text{CO}_3)$, in the powder diffraction study, but if present they are in concentrations of $<5\%$ by volume. It is possible that zemkorite in Pipe-7 could have been derived directly from metasomatic fluids, or by decomposition of one of the components of a natrocarbonate assemblage from the upper mantle. Such a component could be the devitrified Na-rich glass with up to $5\text{ wt}\%$ CaO described by Pyle and Haggerty (1994).

ACKNOWLEDGMENTS

We thank V.P. Dimri for his encouragement, support, and permission to publish this work. We are grateful to K.V. Raghavan for providing the analytical facilities for the characterization of the samples. SEH was supported by a Fulbright Fellowship during his visit to NGRI, Hyderabad and by the National Science Foundation (EAR 01-06187). We thank the reviewers A. Beard and H.L. Barwood for improving the manuscript with their very useful comments and suggestions.

REFERENCES CITED

- Barker, D.S. (1996) Consequences of recycled carbon in carbonatites. *Canadian Mineralogist*, 34, 373–387.
- Bell, K. (1989) Carbonatites Genesis and Evolution, 611 p. Unwin Hyman, London.
- Chalapathi Rao, N.V. (1998) A lithospheric mantle source for the Proterozoic kimberlites and lamproites from the eastern Dharwar Craton, India: evidence from rare earth element inversion modelling. *Current Science*, 74, 777–780.
- Chetty, T.R.K. (1995) Significance of the block rotation model in tectonics and mineralization in Precambrian terrains— an example from the South Indian shield. *Journal of Geodynamics*, 30, 255–266.
- Cooper, A.F. and Gittins, J. (1974) Shortite in kimberlite from the upper Canada gold mine. Ontario: A discussion. *Journal of Geology*, 82, 667–669.
- Cooper, A.F., Gittins, J., and Tuttle, O.F. (1975) The system $\text{Na}_2\text{CO}_3\text{-K}_2\text{CO}_3\text{-CaCO}_3$ at 1 kilobar and its significance in carbonatite petrogeneses. *American Journal of Science*, 275, 534–560.
- Gasparik, T. and Hutchison, M.T. (2000) Experimental evidence for the deep origin of two kinds of inclusions in diamonds from the deep mantle. *Earth and Planetary Science Letters*, 181, 103–114.
- Guptasarma, D., Chetty, T.R.K., Murthy, D.S.N., Rao, A.V.R., Venkatnarayana, B., and Baker, N.A. (1986) Discovery of a new kimberlite pipe in Andrapradesh by stream sediment sampling. *Journal of the Geological Society of India*, 27, 313–316.
- Haggerty, S.E. (1986) Diamond genesis in a multiply constrained model. *Nature*, 320, 34–38.
- (1989) Mantle metasomes and the kinship between carbonatites and kimberlites. In K. Bell, Ed., *Carbonatites Genesis and Evolution*, p. 546–560. Unwin Hyman, London.
- (1995) Upper mantle mineralogy. *Journal of Geodynamics*, 20, 331–364.
- Hazen, R.M. (1985) Comparative crystal chemistry and the polyhedral approach. In S.W. Kieffer and A. Navrotsky, Eds., *Microscopic to Macroscopic: Atomic Environments to Mineral Thermodynamics*, 14, 317–346. Reviews in Mineralogy, Mineralogical Society of America, Washington, D.C.
- Holland, T.J.B. and Powell, R. (1990) An enlarger and updated internally consistent thermodynamic data set with uncertainties and correlations: The system $\text{K}_2\text{O-Na}_2\text{O-CaO-MgO-MnO-FeO-Fe}_2\text{O}_3\text{-Al}_2\text{O}_3\text{-TiO}_2\text{-SiO}_2\text{-C-H}_2\text{-O}_2$. *Journal of Metamorphic Geology*, 8, 89–124.
- Izraeli, E.S., Harris, J.W., and Navon, O. (2001) Brine inclusions in diamond: a new upper mantle fluid. *Earth and Planetary Science Letters*, 187, 323–332.
- Jambor, J.L. and Grew, E.S. (1990) New Minerals. *American Mineralogist*, 75, 931–937.
- Jones, G.C. and Jackson, B. (1993) Infrared transmission spectra of carbonate minerals. Chapman and Hall, London.
- Kononov, S.P. and Solomonik, V.G. (1983) Theoretical study of the electronic and geometric structure, force fields, and vibrational spectra of free BO_2^- , NO_3^- and CO_3^{2-} ions. *Journal of Physical Chemistry*, 57, 384–386.
- Kraft, S., Knittle, E., and Williams, Q. (1991) Carbonate stability in the Earth's mantle: A vibrational spectroscopic study of aragonite and dolomite at high-pressures and temperatures. *Journal of Geophysical Research*, 96B, 17997–18009.
- Kumar, A., Padmakumari, V.M., Dayal, A.M., Murthy, D.S.N., and Gopalan, K. (1993) Rb-Sr ages of Proterozoic kimberlites of India, evidence for contemporaneous emplacement. *PreCambrian Research*, 62, 227–237.
- La Iglesia, A. and Felix, J.F. (1994) Estimation of thermodynamic properties of mineral carbonates at high and low temperatures from the sum of polyhedral contributions. *Geochimica Cosmochimica Acta*, 58, 3983–3991.
- Luth, R.W. (2001) Experimental determination of the reaction aragonite+magnesite = dolomite at 5 to 9 GPa. *Contribution to Mineralogy and Petrology*, 141, 222–232.
- McMillan, P.F. and Hofmeister, A.M. (1988) Infrared and Raman spectroscopy In F.C. Hawthorne, Ed., *Spectroscopic Methods in Mineralogy and Geology*, 18, 99–159. Reviews in Mineralogy, Mineralogical Society of America, Washington, D.C.
- Mukherjee, A. (2000) Oxygen fugacity and geochemical characteristics of some of the Proterozoic Indian Kimberlites. In S.K. Verma, Ed., *Proceeding of Workshop on Status, Complexities, and Challenges of Diamond Exploration in India*. U.S. Educational Foundation in India, Raipur p. 31–39.
- Navrotsky, A. (1995) Thermodynamic properties of minerals. In *Mineral Physics and Crystallography: A Handbook of Physical Constants*, AGU Reference Shelf 2, 18–28.
- Parthasarathy, G., Chetty, T.R.K., and Tajudeen, S. (2001) High-temperature heat capacity and thermal expansion studies of pyrope-rich garnet from Venkatempalle (pipe-7) kimberlite. *Deep Continental Studies in India (DST, India)* 11, 14–15.
- Pyle, J. and Haggerty, S.E. (1994) Silicate-carbonate liquid immiscibility in upper-mantle eclogites: implications for natrosilicic and carbonatitic conjugate melts. *Geochimica Cosmochimica Acta*, 58, 2997–3011.
- Rao, J.M. and Charan, S.N. (1993) Petrography and geochemistry of the pipe-7 kimberlite, Ananthapur district, Andhra Pradesh, India. *Journal of the Geological Society of India*, 42, 469–480.
- Robie, R.A., Hemingway, B.S., and Fisher, J.R. (1978) Thermodynamic properties of minerals and related substances at 298.15 K and 1 bar (10^5 Pa) and at higher temperatures. *United States Geological Survey Bulletin*, 1452, 456 p.
- Schrauder, M., Navon, O., Szafrank, D., Kaminsky, F.V., and Galimov, E.M. (1994) Fluids in Yakutian and Indian diamonds. *Mineralogical Magazine*, 58A, 813–814.
- Watkinson, D.H. and Chao, G.Y. (1973) Shortite in kimberlite from the upper Canada gold mine. *Ontario Journal of Geology*, 81, 229–233.
- White, W.B. (1974) The carbonate minerals. In V.C., Farmer, Ed., *The infrared spectra of minerals*, Monograph 4, 227–284. Mineral Society of London.
- Yegorov, N.K., Ushchapovskaya, Z.F., Kashayev, A.A., Bogdanov, G.V., and Sizykh Yu, I. (1988) Zemkorite, a new carbonate from kimberlites of Yakutia. *Doklady Akad. Nauk. SSSR* 30, 188–193.

MANUSCRIPT RECEIVED AUGUST 27, 2001

MANUSCRIPT ACCEPTED JUNE 18, 2002

MANUSCRIPT HANDLED BY CELIA MERZBACHER